HMG Advance Access published April 25, 2012

Human Molecular Genetics, 2012 **1–10**
doi:10.1093/hmg/dds145

Ryanodine receptor antagonists adapt NPC1 proteostasis to ameliorate lipid storage in Niemann–Pick type C disease fibroblasts

Ting Yu[1], Chan Chung[1], Dongbiao Shen[2], Haoxing Xu[2] and Andrew P. Lieberman[1,*]

[1]Department of Pathology and [2]Department of Molecular, Cellular and Developmental Biology, University of Michigan Medical School, Ann Arbor, MI 48109, USA

Received January 20, 2012; Revised March 13, 2012; Accepted April 9, 2012

Niemann–Pick type C disease is a lysosomal storage disorder most often caused by loss-of-function mutations in the *NPC1* gene. The encoded multipass transmembrane protein is required for cholesterol efflux from late endosomes and lysosomes. Numerous missense mutations in the *NPC1* gene cause disease, including the prevalent I1061T mutation that leads to protein misfolding and degradation. Here, we sought to modulate the cellular proteostasis machinery to achieve functional recovery in primary patient fibroblasts. We demonstrate that targeting endoplasmic reticulum (ER) calcium levels using ryanodine receptor (RyR) antagonists increased steady-state levels of the NPC1 I1061T protein. These compounds also promoted trafficking of mutant NPC1 to late endosomes and lysosomes and rescued the aberrant storage of cholesterol and sphingolipids that is characteristic of disease. Similar rescue was obtained using three distinct RyR antagonists in cells with missense alleles, but not with null alleles, or by over-expressing calnexin, a calcium-dependent ER chaperone. Our work highlights the utility of proteostasis regulators to remodel the protein-folding environment in the ER to recover function in the setting of disease-causing missense alleles.

INTRODUCTION

Niemann–Pick type C disease is an autosomal recessive neurodegenerative disorder for which there is no effective treatment (1). Mutations in either of two genes, *NPC1* (2) or *NPC2* (3), disrupt efflux of cholesterol from late endosomes and lysosomes and trigger a clinically heterogeneous phenotype that invariably includes severe neurological dysfunction and early death (4). Most cases of Niemann–Pick C are caused by mutations in *NPC1*, a widely expressed gene encoding a multipass transmembrane glycoprotein localized to late endosomes and lysosomes (5–8). Genetic studies in mice have established that loss of Npc1 in neurons is necessary and sufficient to mediate CNS disease (9–12). Despite our growing understanding of disease pathogenesis, strategies to treat the severe, progressive neurodegeneration that is characteristic of this disorder have remained elusive.

The approach to treating Niemann-Pick C patients is complicated by the genetics of the disease. Over 240 sequence variants in the *NPC1* gene have been identified, with reported nucleotide changes occurring in all 25 exons and 14 introns. Disease-causing mutations are scattered throughout the gene, rather than clustering in a single functional domain such as the sterol-sensing region (13). Furthermore, despite heterogeneity in clinical presentation, genotype–phenotype correlations have yielded limited information (14), and the functions of most regions of the protein remain poorly understood. Despite these challenges, it has become clear that disease is most commonly caused by missense mutations that lead to non-conservative amino acid substitutions (13). The mechanism by which a missense mutation leads to loss of functional NPC1 has been studied in detail for one particular mutant, I1061T, which is found in ~20% of patients of western European ancestry (15). This mutation leads to misfolding of the NPC1 protein in the endoplasmic reticulum (ER) and to its subsequent degradation by the proteasome (16). That mutant NPC1 is synthesized but fails to fold properly raises the possibility that remodeling of the protein-folding environment in the ER may enable the protein to attain its proper conformation. This approach was first pioneered in studies of

*To whom correspondence should be addressed at: Department of Pathology, University of Michigan Medical School, 3510 MSRB1, 1150 West Medical Center Drive, Ann Arbor, MI 48109-0605, USA. Tel: +1 7346474624; Fax: +1 7346153441; Email: liebermn@umich.edu

Gaucher disease, another lysosomal storage disorder where missense mutations lead to the loss of functional enzyme, glucocerebrosidase (17–19). Although misfolded NPC1 I1061T is subject to ER-associated degradation, if the mutant protein is over-expressed *in vitro*, some of it transits to late endolysosomes/lysosomes and is functional (16). This suggests that strategies to promote proper folding and trafficking may enable functional recovery of the I1061T mutant.

Here, we present evidence that ryanodine receptor (RyR) antagonists are potent modulators of mutant NPC1 folding and trafficking. We use these small molecules to elevate ER calcium stores and target the proteostasis network, and show that this increases steady-state levels of NPC1 I1061T protein, promotes its trafficking to late endosomes and lysosomes and ameliorates both the cholesterol storage and sphingolipid trafficking defects in patient fibroblasts. Our findings indicate that proteostasis regulators can be effective therapeutic reagents for Niemann–Pick type C disease caused by missense mutations.

RESULTS

The RyR antagonist DHBP increases steady-state levels of NPC1 I1061T

To confirm that *NPC1* missense mutations lead to degradation of the mutant, misfolded protein, primary fibroblasts from patients were treated with MG132, an inhibitor of protein degradation through the proteasome, and NPC1 protein levels were determined by western blot (Fig. 1A). Four patient-derived fibroblast lines were examined, three of which carried at least one copy of the I1061T allele. In each case, basal NPC1 protein levels were lower than in controls and were increased after treatment with MG132. These data are consistent with prior reports that *NPC1* missense mutants, including I1061T, are rapidly degraded by the proteasome (16).

To test the hypothesis that elevating ER calcium stores will remodel the protein-folding environment so that it is more favorable to mutant NPC1, we examined the effects of several well-characterized RyR antagonists. As this receptor is a channel that mediates calcium efflux from the ER lumen, RyR antagonists are known to increase ER calcium concentration (18). We initially tested these small molecules on patient fibroblasts carrying one or two copies of the I1061T allele since this mutant encodes a functionally active protein (16). We identified the RyR antagonist DHBP (1,1′-diheptyl-4,4′-bipyridium) as a potent inducer of NPC1 protein, increasing its steady-state level in a dose-dependent manner (Fig. 1B). This occurred without altering *NPC1* mRNA levels (Fig. 1C), suggesting that DHBP enhanced NPC1 protein stability, an interpretation supported by cycloheximide chase studies (Fig. 1D).

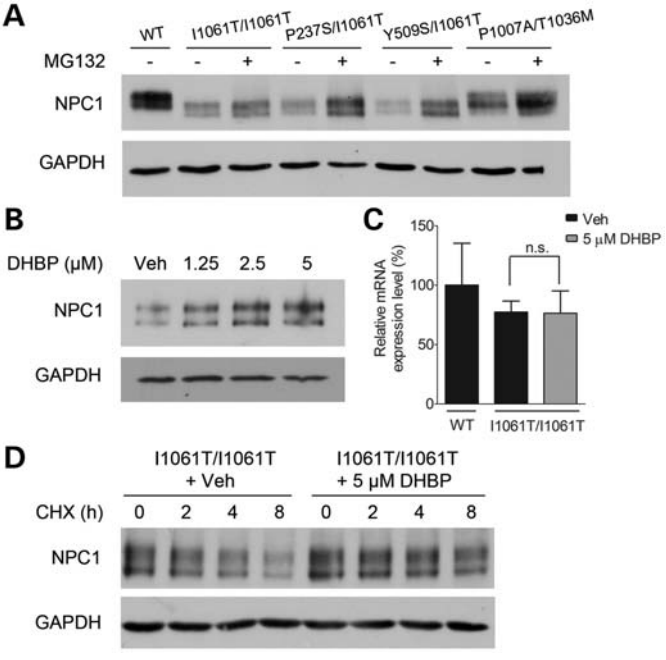

Figure 1. NPC1 I1061T is degraded by the proteasome, and the RyR antagonist DHBP increases its steady-state level. (**A**) Primary human fibroblasts with different NPC1 mutations were treated with 10 μM MG132 or vehicle (DMSO) for 24 h, and cell lysates were examined by western blot for the expression of NPC1 (top). GAPDH controls for loading (bottom). (**B**) NPC1 I1061T homozygous fibroblasts were treated with increasing concentrations of DHBP or vehicle for 7 days, and cell lysates were analyzed by western blot for the expression of NPC1 (top). GAPDH controls for loading (bottom). (**C** and **D**) NPC1 I1061T homozygous or control fibroblasts were treated with 5 μM DHBP or vehicle for 5 days. (C) *NPC1* mRNA levels were determined by quantitative real-time RT-PCR (mean ± SD). n.s., not significant. (D) Cells were treated with 30 μg/ml cycloheximide (CHX) for times indicated and lysates analyzed by western blot for NPC1 expression.

DHBP promotes intracellular trafficking of NPC1 I1061T

Next we sought to determine whether the increase of NPC1 protein levels mediated by DHBP treatment was accompanied by trafficking of mutant NPC1 to its normal intracellular location in late endosomes and lysosomes. We first employed a biochemical approach to analyze NPC1 trafficking by treating cell lysates with endoglycosidase H (Endo H) or peptide: *N*-glycosidase F (PNGase F). Endo H removes high mannose type N-linked glycans from proteins in the ER, but cannot cleave them after the oligosaccharide chain is further modified in the medial Golgi. Therefore, resistance to Endo H digestion indicates that the glycoprotein has trafficked beyond the ER in the secretory pathway. PNGase F is a glycoamidase that removes all types of N-linked glycans and enables visualization of the unmodified protein. In control fibroblasts, wild-type (WT) NPC1 was present as an Endo H-resistant, slow migrating species (Fig. 2A), indicating that the protein was properly folded and efficiently transported out of ER. In contrast, NPC1 I1061T was present as an Endo H-sensitive, more rapidly migrating species (Fig. 2A), consistent with the notion that the mutant protein was retained in the ER prior to its degradation. However, after DHBP treatment, NPC1 I1061T showed a detectable increase in the Endo H-resistant band (Fig. 2A and B), suggesting that a small portion of the mutant protein folded correctly and fluxed through the Golgi.

To gain support for this interpretation, we visualized NPC1 protein by immunofluorescence and assessed its co-localization by confocal microscopy with LAMP1, a marker of late endosomes and lysosomes. In control

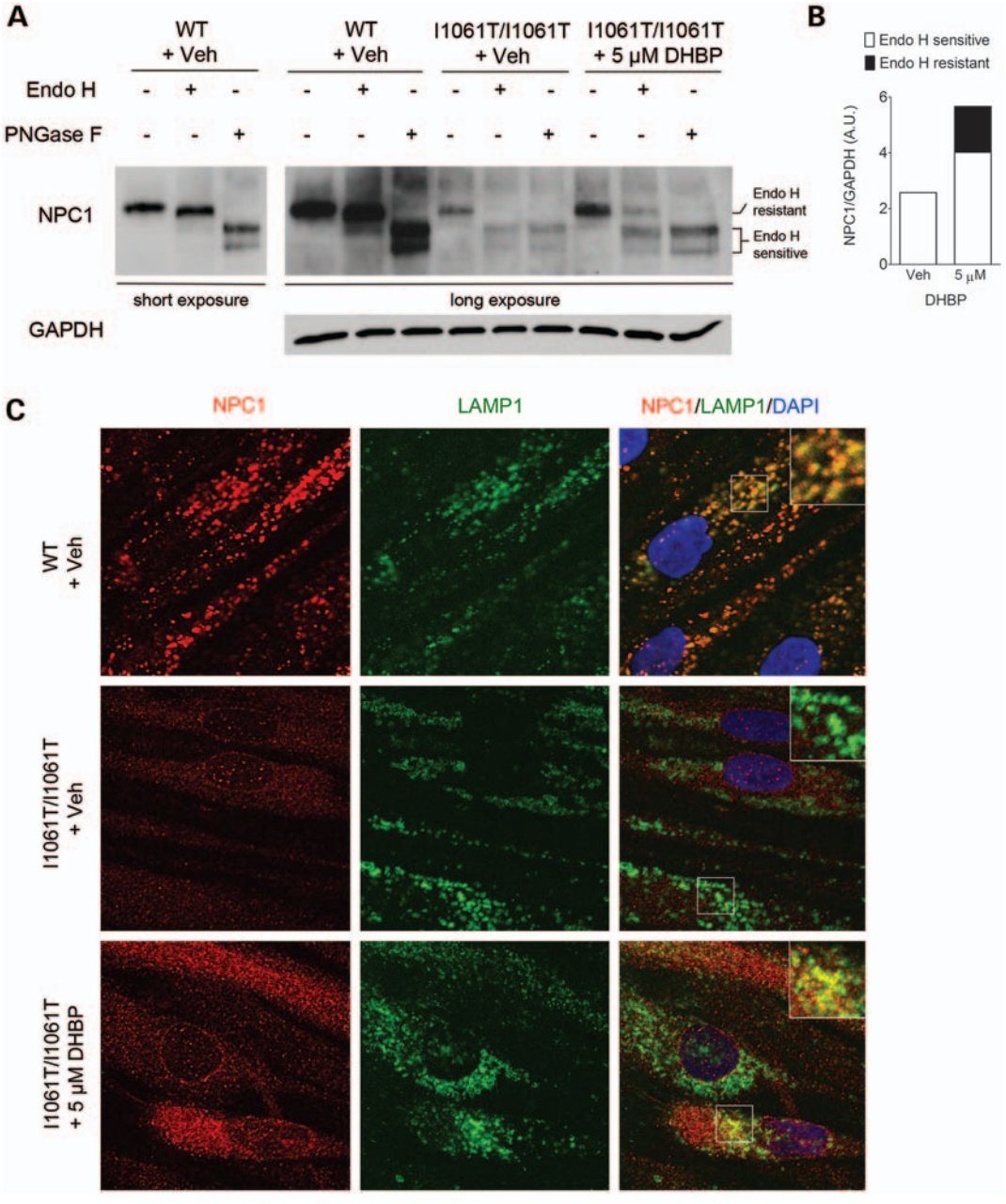

Figure 2. DHBP promotes intracellular trafficking of NPC1 I1061T. (**A**) NPC1 I1061T homozygous and control (WT) fibroblasts were treated with 5 μM DHBP or vehicle for 7 days. Lysates were digested with Endo H or PNGase F for the detection of the post-ER glycoform of NPC1 protein (Endo H resistant). (**B**) Quantification of Endo H-sensitive and Endo H-resistant forms of NPC1 protein levels, as described in (A). A.U., arbitrary units. (**C**) Confocal microscopy shows localization of NPC1 (red) and LAMP1 (green) in NPC1 I1061T homozygous fibroblasts and controls treated with 5 μM DHBP or vehicle for 5 days. Inserts show higher magnification of the boxed regions.

fibroblasts, WT NPC1 protein was present in cytoplasmic puncta that co-localized with LAMP1 (Fig. 2C, top), whereas in mutant fibroblasts, NPC1 I1061T showed a weak and diffuse staining pattern that did not show LAMP1 co-localization (Fig. 2C, middle). However, DHBP treatment increased the staining intensity of the mutant protein and resulted in focal co-localization with LAMP1 (Fig. 2C, bottom). The degree of co-localization between NPC1 I1061T and LAMP1 was quantified by calculating the Pearson correlation coefficient (R_p); this was significantly increased (0.287 ± 0.059 versus 0.392 ± 0.110, $P < 0.05$) following DHBP treatment. We considered the possibility that this effect might be due to diminished degradation of the Endo H-resistant species in lysosomes after DHBP treatment. However, we found that the Endo H-resistant species was relatively insensitive to the lysosomal inhibitor chloroquine (Supplementary Material, Fig. S1), consistent with prior studies demonstrating that NPC1 I1061T is not significantly degraded

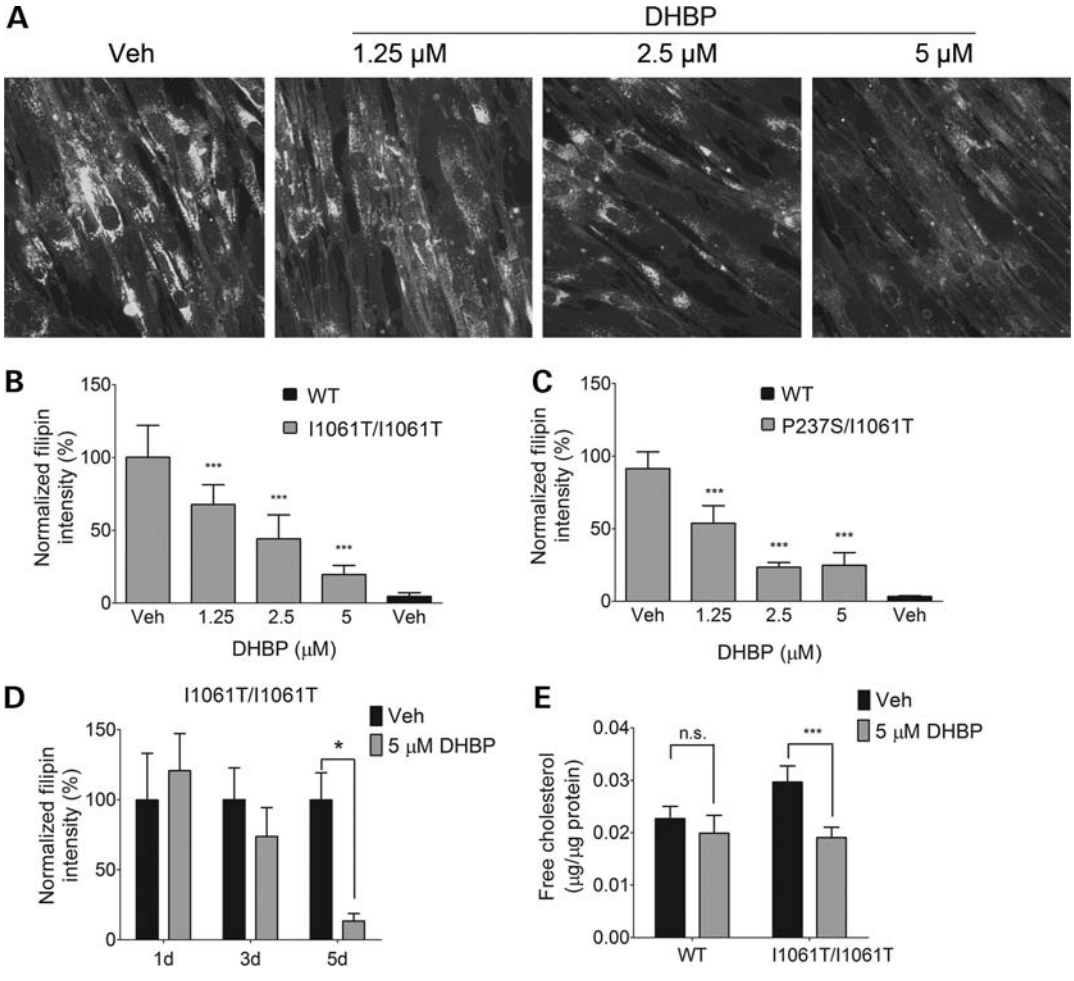

Figure 3. DHBP ameliorates cholesterol storage in NPC1 I1061T fibroblasts. (**A** and **B**) NPC1 I1061T homozygous fibroblasts were treated with increasing concentrations of DHBP for 5 days and then stained for unesterified cholesterol using filipin. Representative images are shown in (A). Quantification of filipin intensity is shown in (**B**), and is reported in comparison with controls. Data are mean ± SD. $^{***}P < 0.001$. (**C**) NPC1 P237S/I1061T fibroblasts were treated with increasing concentrations of DHBP for 5 days, stained with filipin and quantified (mean ± SD). $^{***}P < 0.001$. (**D**) Quantification of filipin staining of NPC1 I1061T homozygous fibroblasts treated with 5 μM DHBP or vehicle for the indicated times (mean ± SD). $^{*}P < 0.05$. (**E**) NPC1 I1061T homozygous and control fibroblasts were treated with DHBP or vehicle for 5 days. Total free cholesterol was measured by Amplex Red cholesterol assay (mean ± SD). n.s., not significant, $^{***}P < 0.001$.

in the lysosome (16). We conclude that DHBP promotes intracellular trafficking of a fraction of the mutant NPC1 protein to late endosomes and lysosomes.

DHBP ameliorates lipid storage in NPC1 I1061T fibroblasts

To determine the extent to which elevated NPC1 protein levels and enhanced localization to late endosomes and lysosomes were associated with functional recovery, we used quantitative filipin microscopy to evaluate the accumulation of unesterified cholesterol, a biochemical hallmark of NPC1-deficient cells. Treatment with DHBP for 5 days significantly decreased filipin staining in fibroblasts homozygous for the NPC1 I1061T allele in a dose-dependent manner (Fig. 3A and B), demonstrating that the treatment diminished lipid storage over the same concentration range that it increased steady-state NPC1 protein levels. Similar results were obtained using an independent line of patient fibroblasts that was a compound heterozygote for the P237S and I1061T alleles (Fig. 3C). Kinetic analysis established that 5 days of treatment was required for DHBP to exert its beneficial effect (Fig. 3D), likely reflecting time required for protein transit through the secretory pathway and then clearance of accumulated lipids. We confirmed these observations using an independent assay to measure total free cholesterol in whole-cell lysates. Compared with controls, NPC1 I1061T homozygotes showed elevated free cholesterol that was corrected to near-WT levels following treatment with DHBP (Fig. 3E).

In addition to the storage of unesterified cholesterol, NPC1-deficient cells also display aberrant sphingolipid trafficking. In control fibroblasts, BODIPY-lactosylceramide (BODIPY-LacCer), a synthetic, fluorescent sphingolipid analog, is targeted to the Golgi after endocytosis, but accumulates in endosomes and lysosomes of NPC1-deficient cells (20,21). We evaluated the intracellular trafficking of BODIPY-LacCer in cells homozygous for the NPC1 I1061T

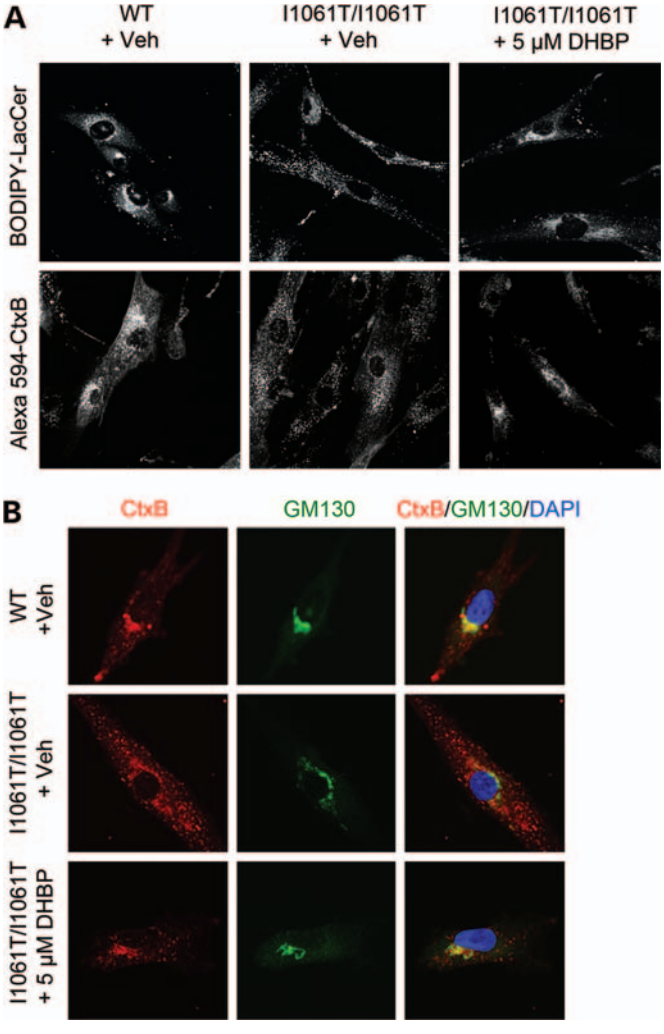

Figure 4. DHBP corrects sphingolipid trafficking in NPC1 I1061T fibroblasts. (**A**) NPC1 I1061T homozygous fibroblasts and controls were treated with 5 μM DHBP or vehicle for 7 days and then pulse-labeled with BODIPY-LacCer (upper panel) or Alexa 594-CtxB (lower panel) to assess intracellular sphingolipid trafficking. (**B**) NPC1 I1061T homozygous fibroblasts and controls were treated with 5 μM DHBP or vehicle for 7 days. Cells were pulse-labeled with Alexa 594-CtxB, followed by immunofluorescence staining with the Golgi marker GM130. Confocal microscopy was used to assess co-localization.

allele and found that treatment with DHBP for 5 days corrected its transport to the Golgi (Fig. 4A, top). Similarly, Alexa fluor 594-labeled cholera toxin subunit B (Alexa 594-CtxB), which binds to endogenous monosialotetrahexosylganglioside (GM1) at the cell surface, is transported to the Golgi after internalization in control fibroblasts, but accumulates in endosomes of NPC1 mutant cells (22,23). Treatment with DHBP also corrected this GM1 trafficking defect (Fig. 4A and B, bottom). Taken together, these data demonstrate that DHBP rescues both the cholesterol and sphingolipid storage phenotypes in mutant NPC1 fibroblasts.

Not all compounds that target calcium levels ameliorated lipid trafficking defects in NPC1-deficient cells. In addition to RyR antagonists, L-type voltage-gated calcium channel blockers modulate ER calcium stores by reducing calcium-induced calcium release. As these small molecules modulate proteostasis of mutant glucocerebrosidase in fibroblasts (17,18), we tested their ability to restore mutant NPC1 function. Treatment with diltiazem or verapamil, two L-type calcium channel blockers, resulted in a dose-dependent increase in the steady-state level of NPC1 protein in fibroblasts homozygous for the NPC1 I1061T allele (Fig. 5A). However, this was not associated with an increase in the Endo H-resistant species (Fig. 5B) and was unexpectedly accompanied by an exacerbation of the cholesterol storage phenotype (Fig. 5C and D). This may reflect inhibitory effects of these compounds on intracellular lipid metabolism, such as cholesterol esterification (24), and off-target effects on other ion channels, or other, less well-characterized actions. These observations focused our efforts on defining the mechanism by which RyR antagonists exerted therapeutic effects.

RyR antagonists act through NPC1 protein-dependent mechanisms

To test our working model that DHBP targets RyRs to enhance mutant NPC1 proteostasis, we examined the effects of additional RyR antagonists on cholesterol storage in fibroblasts homozygous for the NPC1 I1061T allele. Similar to DHBP, both ruthenium red and dantrolene reduced the intensity of filipin staining (Fig. 6A and B). In contrast, DHBP was ineffective at altering filipin staining of patient fibroblasts carrying two null alleles (*NPC1* 1628delC) of the *NPC1* gene (Fig. 6C), confirming that NPC1 protein was necessary for its beneficial effects. We also considered the possibility that DHBP exerted its therapeutic effects by targeting other calcium channels, such as those localized to lysosomes that have been implicated in regulating exocytosis (25). However, we found that DHBP did not trigger the release of lysosomal calcium through the TRPML1 channel (Fig. 6D). To further test the notion that these small molecules facilitated calcium-dependent ER proteostasis, we transiently over-expressed calnexin (Fig. 7A), a calcium-dependent ER chaperone. We found that calnexin over-expression was sufficient to promote the appearance of Endo H-resistant NPC1 species (Fig. 7B) and significantly reduce filipin staining of NPC1 mutant fibroblasts (Fig. 7C and D). Taken together, our data demonstrate that genetic or pharmacological manipulation of the protein-folding environment within ER modulates the stability, trafficking and function of mutant NPC1 to yield a functional recovery.

DISCUSSION

Our findings demonstrate that RyR antagonists ameliorate lipid storage in patient fibroblasts expressing NPC1 I1061T by modifying mutant NPC1 proteostasis. By diminishing the activity of this calcium efflux channel, the mutant protein is stabilized, its transit through the secretory pathway to late endosomes and lysosomes is promoted and the storage of unesterified cholesterol and sphingolipids is alleviated. Similar effects were observed by transiently over-expressing calnexin. Our data are consistent with the model that DHBP and other RyR antagonists inhibit the spontaneous activity of RyRs to increase ER luminal calcium concentration, which in turn increases the activity of calcium-dependent chaperones

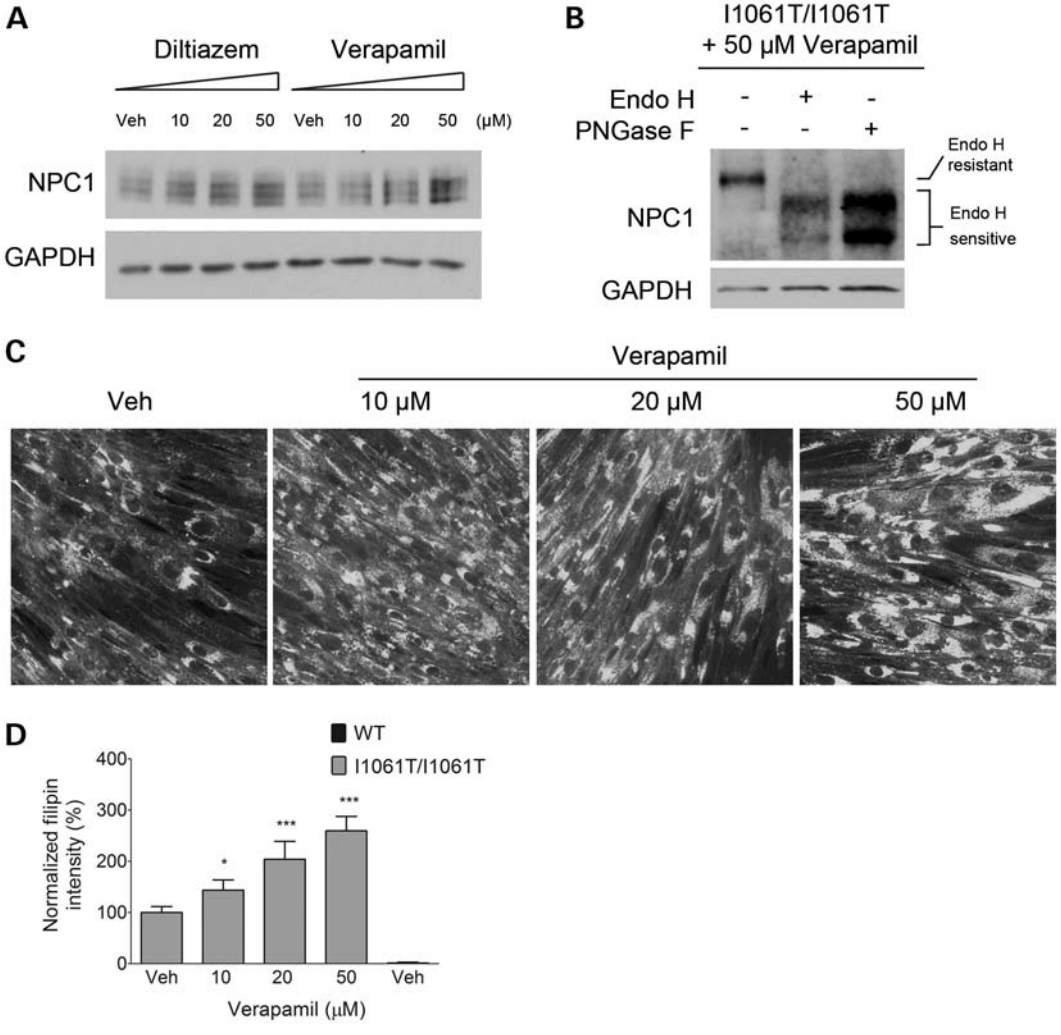

Figure 5. L-type calcium channel blockers exacerbate cholesterol storage in NPC1 I1061T fibroblasts. (**A**) Cells were treated with increasing concentrations of diltiazem or verapamil for 7 days, and lysates were examined by western blot for the expression of NPC1 (top) and GAPDH (bottom). (**B**) NPC1 I1061T homozygous fibroblasts were treated with 50 μM verapamil for 7 days. Lysates were digested with Endo H or PNGase F for the detection of the post-ER glycoform of NPC1 protein (Endo H resistant). (**C** and **D**) Fibroblasts were treated with increasing concentrations of verapamil for 7 days and then stained with filipin. Representative images are shown in (C). Quantification of filipin intensity is shown in (D), and for comparison, filipin intensity of WT fibroblasts is included (mean ± SD). $^{*}P < 0.05$, $^{***}P < 0.001$.

such as calnexin. Although RyR antagonists may have yet uncharacterized off-target partners in the cell, and, likewise, calnexin over-expression may invoke effects independent of its activity as an ER chaperone, the combination of these two approaches provides strong, complementary evidence for the idea that modulating the ER protein folding environment enhances proteostasis of mutant NPC1. Other calcium-dependent chaperones are also present in the ER lumen, including BiP and calreticulin, and their roles in NPC1 proteostasis remains to be defined. Although treatment with DHBP or over-expression of calnexin promoted intracellular trafficking of only a small fraction of the mutant protein, they triggered a significant decrease in cholesterol storage, indicating that relatively low levels of recovered protein have marked functional effects.

Treatment of the severe, progressive neurological impairment that is characteristic of Niemann–Pick C disease remains elusive. Miglustat, the only approved treatment for this disorder, may stabilize the progression of neurological symptoms in some Niemann–Pick C patients, but is less effective for others (26–28). Compelling data demonstrate that cyclodextrin, a compound that circumvents NPC1/NPC2 to clear lipid storage from NPC lysosomes (29,30), delays neurodegeneration in Npc1-deficient mice (31–34). However, its limited ability to cross the blood–brain barrier poses therapeutic challenges and suggests that complementary approaches will be beneficial. Recent studies identified HDAC inhibitors as small molecules that alleviate lipid storage in patient fibroblasts (35,36). Our findings add RyR antagonists to this list of compounds with the potential to provide therapeutic benefit to some patients with Niemann–Pick C disease. We note that one of the RyR antagonists tested and proven effective here, dantrolene, is used clinically. Determining the extent to which this compound, or others,

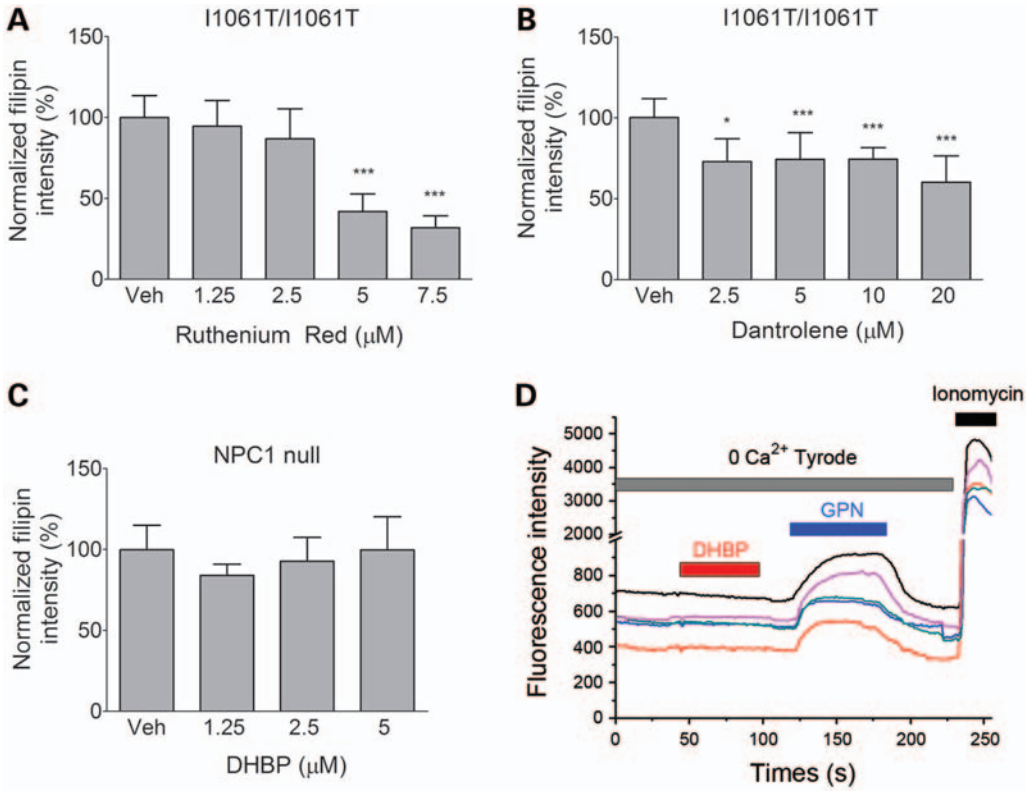

Figure 6. RyR antagonists reduce cholesterol storage in *NPC1* missense mutant fibroblasts. (**A** and **B**) NPC1 I1061T homozygous fibroblasts were treated with ruthenium red, dantrolene or vehicle for 5 days, stained with filipin and quantified (mean ± SD). $^{*}P < 0.05$, $^{***}P < 0.001$. (**C**) Quantification of filipin intensity in NPC1 null fibroblasts (1628delC) treated with DHBP or vehicle for 5 days (mean ± SD). $P > 0.05$. (**D**) CHO cells were transfected with a genetically encoded Ca^{2+} indicator (GCaMP3) fused to the N-terminus of TRPML1 (40). TRPML1-mediated lysosomal Ca^{2+} release, as measured by GCaMP3 fluorescence, was examined after sequential application of 50 μM DHBP (in 0 Ca^{2+} tyrode with <10 nM Ca^{2+}), 200 μM glycyl-L-phenylalanine 2-naphthylamide (GPN, in 0 Ca^{2+} tyrode with <10 nM Ca^{2+}), a cathepsin C substrate that induces lysosomal rupture (41), and 1 μM ionomycin (in tyrode with 2 mM Ca^{2+}). Shown are data from five representative cells, with each cell tracing in a different color.

alters NPC1 proteostasis in more complex disease models is an important future objective.

Our data extend observations from Gaucher disease fibroblasts (17–19), highlighting the utility of proteostasis regulators in patients with disease-causing missense mutations. Here, we have demonstrated that this strategy is also applicable to a multipass transmembrane protein that traffics through the secretory pathway. As other NPC1 missense mutations also lead to protein misfolding and degradation, we suggest that this strategy may be applicable to the subset of disease-causing mutations where function is retained. These findings suggest that small molecules that remodel the protein-folding environment in the ER may be therapeutically beneficial for some Niemann–Pick C patients, and potentially, for patients with other disorders caused by missense mutations.

MATERIALS AND METHODS

Reagents

DHBP (180858), dantrolene (D9175), diltiazem (D2521), verapamil (V4629), filipin (F9765) and cycloheximide (C4859) were from Sigma. Chloroquine (193919) and ruthenium red (156565) were from MP Biomedical. Ruthenium red and dantrolene were diluted in DMSO, and other channel blockers were diluted in water. BODIPY FL C5-lactosylceramide complexed to BSA (BODIPY-LacCer) and cholera toxin subunit B, Alexa Fluor 594 conjugate (Alexa 594-CtxB), were from Invitrogen. The calnexin-3XFlag expression plasmid was from GeneCopoeia.

Cell culture and transfection

Human dermal fibroblast lines GM08399 (healthy control) and GM18453 (NPC1 I1061T/I1061T), GM03123 (NPC1 P237S/I1061T), GM17926 (NPC1 Y509S/I1061T), GM17912 (NPC1 P1007A/T1036M) were from Coriell Cell Repositories. Human dermal fibroblasts homozygous for the NPC11628delC allele (NIH 98.016) (37) were a gift from Dr Daniel Ory. Cells were maintained in modified Eagle's medium (MEM, Gibco), supplemented with 15% FBS (Atlanta Biologicals), 10 μg/ml penicillin, 10 μg/ml streptomycin and 2 mM glutamine (Gibco). Control (RA25) CHO cells were a gift from Dr T.Y. Chang, and were maintained in DMEM/F12 (Gibco) supplemented with 10% FBS. Cells were transfected with 3 μg of plasmid by electroporation using a Nucleofector II (Lonza) per manufacturer's instructions.

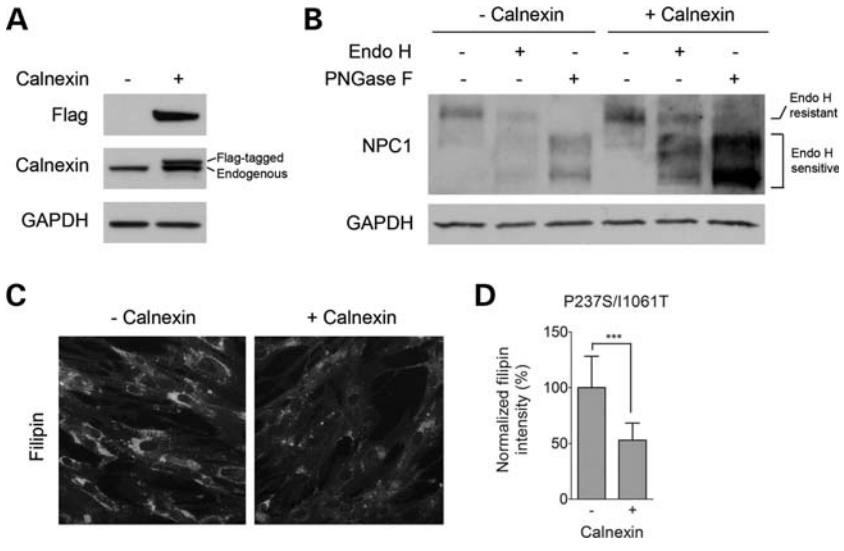

Figure 7. Calnexin over-expression promotes mutant NPC1 proteostasis. (**A**) NPC1 mutant fibroblasts were transiently transfected with 3XFlag-calnexin for 2 days and cell lysates were analyzed by western blot for the expression of Flag (upper) and calnexin (middle). GAPDH (bottom) controls for loading. (**B**) NPC1 P237S/I1061T fibroblasts were transfected to express 3XFlag-calnexin. Lysates were harvested 6 days later and then digested with Endo H or PNGase F for the detection of the post-ER glycoform of NPC1 protein (Endo H resistant). (**C** and **D**) NPC1 P237S/I1061T fibroblasts were stained with filipin 6 days after 3XFlag-calnexin transfection. Representative images are shown in (C). Quantification of filipin intensity is shown in (D), and is reported in comparison with controls. Data are mean ± SD. $^{***}P < 0.001$.

Quantitative filipin staining

Cells were grown on glass chamber slides and stained with filipin as described (38). Images were captured on a Zeiss Axioplan 2 imaging system equipped with a Zeiss AxioCam HRc camera, with a 10× Zeiss EC Plan-NEOFLUAR objective, using the AxioVision 4.8 software. Quantitative analysis of filipin images from more than 5 fields of cells/experiment was performed using the NIH ImageJ software, following the 'LSO compartment ratio assay' method (39). Data reported are from one of three similar experiments.

Amplex Red cholesterol assay

Total free cholesterol levels were determined using the Amplex Red cholesterol assay kit (Invitrogen) per manufacturer's instructions. Results were normalized to protein concentration determined by protein assay (Bio-Rad).

Sphingolipid trafficking

BODIPY-LacCer labeling was performed as described (20). Briefly, cells were washed three times with MEM and then incubated with 5 μM BODIPY LacCer/BSA in MEM containing 1% FBS for 45 min at 37°C. Cells were then washed three times with MEM containing 1% FBS and incubated for another 60 min at 37°C. Next, cells were washed three times with DMEM without glucose, and then were back-exchanged at 4°C for 6 × 10 min with DMEM without glucose containing 5% defatted BSA. Alexa 594 CtxB labeling was carried out similarly, except that Alexa 594 CtxB (1:1000) was used in the pulse labeling step and the cells were chased for 2 h at 37°C. In some experiments, after Alexa 594 CtxB labeling, cells were fixed with 4% paraformaldehyde and incubated with the rabbit anti-GM130 antibody (Abcam, 1:200) to visualize the Golgi apparatus. Confocal microscopy was performed using an Olympus FluoView 500 Confocal Microscope system, with a 60× WPSF water immersion objective, using the Olympus FluoView software.

Immunofluorescence

Cells grown on cover slips were washed with PBS and fixed with methanol for 30 min. Cells were subsequently washed with PBS and incubated with blocking buffer containing 5% donkey serum, 1% BSA and 0.2% Triton X for 1 h, followed by incubation with primary antibodies in buffer containing 1.25% donkey serum, 0.25% BSA and 0.05% Triton X at 4°C overnight. Antibodies used were rabbit anti-NPC1 (Abcam, 1:500) and mouse anti-LAMP1 H4A3 (Developmental Studies Hybridoma Bank, 1:50). Next, cells were washed with PBS containing 0.05% Triton X, incubated with Alexa fluor-conjugated secondary antibodies (Invitrogen) and then washed with PBS containing 0.05% Triton X. Cover slips were mounted using Vectashield mounting medium with DAPI (Vector Laboratories). Confocal microscopy was performed using a Zeiss LSM 510-META Laser Scanning Confocal Microscopy system, with a 63× Zeiss C-Apochromat water immersion objective, NA of 1.2, using the Zeiss LSM 510-META software. For analysis of NPC1 and LAMP1 co-localization, the Pearson correlation coefficient was calculated using NIH ImageJ.

N-linked glycan removal assays and western blot analysis

Cells were harvested, washed with PBS and lysed in RIPA buffer containing Complete Protease Inhibitor Cocktail (Roche) and phosphatase inhibitor (Thermo Scientific). For the cleavage of N-linked glycans, non-denatured protein

samples were treated with PNGase F (NEB) or Endo H (NEB) at 37°C for 3 h in the supplied buffers. For western blot, non-boiled samples were electrophoresed through a 7.5% SDS–polyacrylamide gel or 4–20% Tris–glycine gradient gel (Invitrogen) and transferred to nitrocellulose membranes (Bio-Rad) on a semidry transfer apparatus. Immunoreactivity was detected by TMA-6 (Lumigen) or ECL (Thermo Scientific). Antibodies used were rabbit anti-NPC1 (Abcam) and rabbit anti-GAPDH (Santa Cruz).

Gene expression analysis

Total RNA was isolated from cells, using TRIzol (Invitrogen) as per the manufacturer's protocol. cDNA was synthesized using the High Capacity cDNA Archive Kit (Applied Biosystems). Quantitative real-time RT-PCR was performed on 5 ng of cDNA per reaction, in duplicate. Primers and probes for NPC1 (Hs00264835-m1) and 18S rRNA were purchased from Applied Biosystems. Threshold cycle (C_t) values were determined on an ABI Prism 7900HT Sequence Detection System. Relative expression values were calculated by the standard curve method and normalized to 18S rRNA.

GCaMP3 Ca^{2+} imaging

Eighteen to 24 h after transfection with GCaMP3-ML1 (40), CHO cells were trypsinized and plated onto glass cover slips. The fluorescence intensity at 470 nm was monitored using the EasyRatioPro system. Ionomycin (1 mM) in tyrode was added at the end of all experiments to induce a maximal response for comparison.

Statistics

Statistical significance was assessed by unpaired Student's *t*-test (for comparison of two means) or ANOVA (for comparison of more than two means). The Newman–Keuls *post hoc* test was performed to carry out pairwise comparisons of group means if ANOVA rejected the null hypothesis. Statistics were performed using the software package Prism 5 (GraphPad Software). *P*-values <0.05 were considered significant.

SUPPLEMENTARY MATERIAL

Supplementary Material is available at *HMG* online.

ACKNOWLEDGEMENTS

We thank Dr Daniel Ory for NPC1 1628delC fibroblasts and Dr T.Y. Chang for RA25 CHO cells.

Conflict of Interest statement. None declared.

FUNDING

This work was supported by the National Institutes of Health (NS063967 and NS078526 to A.P.L., and NS062792 to H.X.).

REFERENCES

1. Vanier, M.T. (2010) Niemann-Pick disease type C. *Orphanet. J. Rare Dis.*, **5**, 16.
2. Carstea, E.D., Morris, J.A., Coleman, K.G., Loftus, S.K., Zhang, D., Cummings, C., Gu, J., Rosenfeld, M.A., Pavan, W.J., Krizman, D.B. *et al.* (1997) Niemann-Pick C1 disease gene: homology to mediators of cholesterol homeostasis. *Science*, **277**, 228–231.
3. Naureckiene, S., Sleat, D.E., Lackland, H., Fensom, A., Vanier, M.T., Wattiaux, R., Jadot, M. and Lobel, P. (2000) Identification of HE1 as the second gene of Niemann-Pick C disease. *Science*, **290**, 2298–2301.
4. Higgins, J.J., Patterson, M.C., Dambrosia, J.M., Pikus, A.T., Pentchev, P.G., Sato, S., Brady, R.O. and Barton, N.W. (1992) A clinical staging classification for type C Niemann-Pick disease. *Neurology*, **42**, 2286–2290.
5. Neufeld, E.B., Wastney, M., Patel, S., Suresh, S., Cooney, A.M., Dwyer, N.K., Roff, C.F., Ohno, K., Morris, J.A., Carstea, E.D. *et al.* (1999) The Niemann-Pick C1 protein resides in a vesicular compartment linked to retrograde transport of multiple lysosomal cargo. *J. Biol. Chem.*, **274**, 9627–9635.
6. Higgins, M.E., Davies, J.P., Chen, F.W. and Ioannou, Y.A. (1999) Niemann-Pick C1 is a late endosome-resident protein that transiently associates with lysosomes and the trans-Golgi network. *Mol. Genet. Metab.*, **68**, 1–13.
7. Davies, J.P. and Ioannou, Y.A. (2000) Topological analysis of Niemann-Pick C1 protein reveals that the membrane orientation of the putative sterol-sensing domain is identical to those of 3-hydroxy-3-methylglutaryl-CoA reductase and sterol regulatory element binding protein cleavage-activating protein. *J. Biol. Chem.*, **275**, 24367–24374.
8. Garver, W.S., Heidenreich, R.A., Erickson, R.P., Thomas, M.A. and Wilson, J.M. (2000) Localization of the murine Niemann-Pick C1 protein to two distinct intracellular compartments. *J. Lipid Res.*, **41**, 673–687.
9. Ko, D.C., Milenkovic, L., Beier, S.M., Manuel, H., Buchanan, J. and Scott, M.P. (2005) Cell-autonomous death of cerebellar purkinje neurons with autophagy in Niemann-Pick type C disease. *PLoS Genet.*, **1**, 81–95.
10. Elrick, M.J., Pacheco, C.D., Yu, T., Dadgar, N., Shakkottai, V.G., Ware, C., Paulson, H.L. and Lieberman, A.P. (2010) Conditional Niemann-Pick C mice demonstrate cell autonomous Purkinje cell neurodegeneration. *Hum. Mol. Genet.*, **19**, 837–847.
11. Lopez, M.E., Klein, A.D., Dimbil, U.J. and Scott, M.P. (2011) Anatomically defined neuron-based rescue of neurodegenerative Niemann-Pick type C disorder. *J. Neurosci.*, **31**, 4367–4378.
12. Yu, T., Shakkottai, V.G., Chung, C. and Lieberman, A.P. (2011) Temporal and cell-specific deletion establishes that neuronal Npc1 deficiency is sufficient to mediate neurodegeneration. *Hum. Mol. Genet.*, **20**, 4440–4451.
13. Vanier, M.T. and Millat, G. (2003) Niemann-Pick disease type C. *Clin. Genet.*, **64**, 269–281.
14. Runz, H., Dolle, D., Schlitter, A.M. and Zschocke, J. (2008) NPC-db, a Niemann-Pick type C disease gene variation database. *Hum. Mutat.*, **29**, 345–350.
15. Millat, G., Marcais, C., Rafi, M.A., Yamamoto, T., Morris, J.A., Pentchev, P.G., Ohno, K., Wenger, D.A. and Vanier, M.T. (1999) Niemann-Pick C1 disease: the I1061T substitution is a frequent mutant allele in patients of Western European descent and correlates with a classic juvenile phenotype. *Am. J. Hum. Genet.*, **65**, 1321–1329.
16. Gelsthorpe, M.E., Baumann, N., Millard, E., Gale, S.E., Langmade, S.J., Schaffer, J.E. and Ory, D.S. (2008) Niemann-Pick type C1 I1061T mutant encodes a functional protein that is selected for endoplasmic reticulum-associated degradation due to protein misfolding. *J. Biol. Chem.*, **283**, 8229–8236.
17. Mu, T.W., Fowler, D.M. and Kelly, J.W. (2008) Partial restoration of mutant enzyme homeostasis in three distinct lysosomal storage disease cell lines by altering calcium homeostasis. *PLoS Biol.*, **6**, e26.
18. Ong, D.S., Mu, T.W., Palmer, A.E. and Kelly, J.W. (2010) Endoplasmic reticulum Ca2+ increases enhance mutant glucocerebrosidase proteostasis. *Nat. Chem. Biol.*, **6**, 424–432.
19. Wang, F., Agnello, G., Sotolongo, N. and Segatori, L. (2011) Ca2+ homeostasis modulation enhances the amenability of L444P glucosylcerebrosidase to proteostasis regulation in patient-derived fibroblasts. *ACS Chem. Biol.*, **6**, 158–168.

20. Sun, X., Marks, D.L., Park, W.D., Wheatley, C.L., Puri, V., O'Brien, J.F., Kraft, D.L., Lundquist, P.A., Patterson, M.C., Pagano, R.E. *et al.* (2001) Niemann-Pick C variant detection by altered sphingolipid trafficking and correlation with mutations within a specific domain of NPC1. *Am. J. Hum. Genet.*, **68**, 1361–1372.
21. Chen, C.S., Patterson, M.C., Wheatley, C.L., O'Brien, J.F. and Pagano, R.E. (1999) Broad screening test for sphingolipid-storage diseases. *Lancet*, **354**, 901–905.
22. Choudhury, A., Dominguez, M., Puri, V., Sharma, D.K., Narita, K., Wheatley, C.L., Marks, D.L. and Pagano, R.E. (2002) Rab proteins mediate Golgi transport of caveola-internalized glycosphingolipids and correct lipid trafficking in Niemann-Pick C cells. *J. Clin. Invest.*, **109**, 1541–1550.
23. Sugimoto, Y., Ninomiya, H., Ohsaki, Y., Higaki, K., Davies, J.P., Ioannou, Y.A. and Ohno, K. (2001) Accumulation of cholera toxin and GM1 ganglioside in the early endosome of Niemann-Pick C1-deficient cells. *Proc. Natl Acad. Sci. USA*, **98**, 12391–12396.
24. Dushkin, M.I. and Schwartz, Y.S. (1995) Effect of verapamil and nifedipine on cholesteryl ester metabolism and low-density lipoprotein oxidation in macrophages. *Biochem. Pharmacol.*, **49**, 389–397.
25. Dong, X.P., Wang, X., Shen, D., Chen, S., Liu, M., Wang, Y., Mills, E., Cheng, X., Delling, M. and Xu, H. (2009) Activating mutations of the TRPML1 channel revealed by proline-scanning mutagenesis. *J. Biol. Chem.*, **284**, 32040–32052.
26. Patterson, M.C., Vecchio, D., Prady, H., Abel, L. and Wraith, J.E. (2007) Miglustat for treatment of Niemann-Pick C disease: a randomised controlled study. *Lancet Neurol.*, **6**, 765–772.
27. Wraith, J.E. and Imrie, J. (2009) New therapies in the management of Niemann-Pick type C disease: clinical utility of miglustat. *Ther. Clin. Risk Manag.*, **5**, 877–887.
28. Pineda, M., Perez-Poyato, M.S., O'Callaghan, M., Vilaseca, M.A., Pocovi, M., Domingo, R., Portal, L.R., Perez, A.V., Temudo, T., Gaspar, A. *et al.* (2010) Clinical experience with miglustat therapy in pediatric patients with Niemann-Pick disease type C: a case series. *Mol. Genet. Metab.*, **99**, 358–366.
29. Abi-Mosleh, L., Infante, R.E., Radhakrishnan, A., Goldstein, J.L. and Brown, M.S. (2009) Cyclodextrin overcomes deficient lysosome-to-endoplasmic reticulum transport of cholesterol in Niemann-Pick type C cells. *Proc. Natl Acad. Sci. USA*, **106**, 19316–19321.
30. Rosenbaum, A.I., Zhang, G., Warren, J.D. and Maxfield, F.R. (2010) Endocytosis of beta-cyclodextrins is responsible for cholesterol reduction in Niemann-Pick type C mutant cells. *Proc. Natl Acad. Sci. USA*, **107**, 5477–5482.
31. Griffin, L.D., Gong, W., Verot, L. and Mellon, S.H. (2004) Niemann-Pick type C disease involves disrupted neurosteroidogenesis and responds to allopregnanolone. *Nat. Med.*, **10**, 704–711.
32. Liu, B., Turley, S.D., Burns, D.K., Miller, A.M., Repa, J.J. and Dietschy, J.M. (2009) Reversal of defective lysosomal transport in NPC disease ameliorates liver dysfunction and neurodegeneration in the npc1-/- mouse. *Proc. Natl Acad. Sci. USA*, **106**, 2377–2382.
33. Davidson, C.D., Ali, N.F., Micsenyi, M.C., Stephney, G., Renault, S., Dobrenis, K., Ory, D.S., Vanier, M.T. and Walkley, S.U. (2009) Chronic cyclodextrin treatment of murine Niemann-Pick C disease ameliorates neuronal cholesterol and glycosphingolipid storage and disease progression. *PLoS One*, **4**, e6951.
34. Aqul, A., Liu, B., Ramirez, C.M., Pieper, A.A., Estill, S.J., Burns, D.K., Repa, J.J., Turley, S.D. and Dietschy, J.M. (2011) Unesterified cholesterol accumulation in late endosomes/lysosomes causes neurodegeneration and is prevented by driving cholesterol export from this compartment. *J. Neurosci.*, **31**, 9404–9413.
35. Pipalia, N.H., Cosner, C.C., Huang, A., Chatterjee, A., Bourbon, P., Farley, N., Helquist, P., Wiest, O. and Maxfield, F.R. (2011) Histone deacetylase inhibitor treatment dramatically reduces cholesterol accumulation in Niemann-Pick type C1 mutant human fibroblasts. *Proc. Natl Acad. Sci. USA*, **108**, 5620–5625.
36. Munkacsi, A.B., Chen, F.W., Brinkman, M.A., Higaki, K., Gutierrez, G.D., Chaudhari, J., Layer, J.V., Tong, A., Bard, M., Boone, C. *et al.* (2011) An 'exacerbate-reverse' strategy in yeast identifies histone deacetylase inhibition as a correction for cholesterol and sphingolipid transport defects in human Niemann-Pick type C disease. *J. Biol. Chem.*, **286**, 23842–23851.
37. Frolov, A., Zielinski, S.E., Crowley, J.R., Dudley-Rucker, N., Schaffer, J.E. and Ory, D.S. (2003) NPC1 and NPC2 regulate cellular cholesterol homeostasis through generation of low density lipoprotein cholesterol-derived oxysterols. *J. Biol. Chem.*, **278**, 25517–25525.
38. Pacheco, C.D., Kunkel, R. and Lieberman, A.P. (2007) Autophagy in Niemann-Pick C disease is dependent upon Beclin-1 and responsive to lipid trafficking defects. *Hum. Mol. Genet.*, **16**, 1495–1503.
39. Pipalia, N.H., Huang, A., Ralph, H., Rujoi, M. and Maxfield, F.R. (2006) Automated microscopy screening for compounds that partially revert cholesterol accumulation in Niemann-Pick C cells. *J. Lipid Res.*, **47**, 284–301.
40. Shen, D., Wang, X., Li, X., Zhang, X., Yao, Z., Dibble, S., Dong, X.P., Yu, T., Lieberman, A.P., Showalter, H.D. *et al.* (2012) Lipid storage disorders block lysosomal trafficking by inhibiting a TRP channel and lysosomal calcium release. *Nat. Commun.*, **3**, 731. doi: 10.1038/ncomms1735.
41. Berg, T.O., Stromhaug, P.E., Berg, T. and Seglen, P.O. (1994) Separation of lysosomes and autophagosomes by means of glycyl-phenylalanine-naphthylamide, a lysosome-disrupting cathepsin-C substrate. *Eur. J. Biochem.*, **221**, 595–602.